

# Hydrogeochemical and Isotopic Study of Groundwater in a Semi-arid Region: Yeniceoba Plain (Cihanbeyli-KONYA), Central Anatolia, Turkey

Ayla BOZDAĞ\* and Güler GÖÇMEZ

*Department of Geological Engineering, Selcuk University, 42079 Konya, Turkey*

**Abstract:** Groundwater is the most important source of water supply in the Yeniceoba Plain in Central Anatolia, Turkey. An understanding of the geochemical evolution of groundwater is important for the sustainable development of water resources in this region. A hydrogeochemical investigation was conducted in the Plio-Quaternary aquifer system using stable isotopes ( $\delta^{18}\text{O}$  and  $\delta\text{D}$ ), tritium ( $^3\text{H}$ ), major and minor elements (Ca, Na, K, Mg, Cl,  $\text{SO}_4$ ,  $\text{NO}_3$ ,  $\text{HCO}_3$  and Br) in order to identify groundwater chemistry patterns and the processes affecting groundwater mineralization in this system. The chemical data reveal that the chemical composition of groundwater in this aquifer system is mainly controlled by rock/water interactions including dissolution of evaporitic minerals, weathering of silicates, precipitation/dissolution of carbonates, ion exchange, and evaporation. Based on the values of Cl/Br ratio ( $> 300 \text{ mg/l}$ ) in the Plio-Quaternary groundwater, dissolution of evaporitic minerals in aquifer contributes significantly to the high mineralization. The stable isotope analyses indicate that the groundwater in the system was influenced by evaporation of rainfall during infiltration. Low tritium values (generally  $< 1$  tritium units) of groundwater reflect a minor contribution of recent recharge and groundwater residence times of more than three or four decades.

**Key words:** hydrochemistry, stable isotopes, tritium, Yeniceoba Plain, Central Anatolia

## 1 Introduction

Groundwater resources are of great importance for agricultural, industrial, and domestic needs in arid and semi-arid areas around Central Anatolia where surface waters are scarce or absent. The Yeniceoba plain located in Central Anatolia (Fig. 1) is such an arid and semi-arid region in which groundwater resources are intensively exploited for human needs. Adequate assessment, management, and protection of the available groundwater resources require a thorough understanding of their hydrodynamic and hydrochemical characteristics.

Hydrochemical and isotopic methodologies offer effective tools for solving various problems in hydrology, in particular in the arid and semi-arid regions (Clark and Fritz, 1997; Cook and Herczeg, 2000; Edmunds et al., 2003; Guendouz et al., 2003; Edmunds, 2005). Multi-tracer investigations are commonly used to understand groundwater movement, salinity origin, evaporation processes, and recharge periods (Al-Charideh, 2012). Such information which is needed to improve water resource management strategies is of particular

importance for aquifers located in arid and semi arid areas and characterized by complex lithology. This is the case of the Yeniceoba plain in Central Anatolia.

Groundwater used from the Plio-Quaternary aquifer serves as the main water resource for the region. The shallow wells (defined  $< 30 \text{ m}$ ) are extremely exhausted due to increasing water demands having the region suffer from a serious shortage of groundwater resources. As a result, many deep wells (up to  $150 \text{ m}$ ) have been drilled and the water extracted from these deep wells has been used for domestic, industrial, and especially irrigation needs. However, much of this water supply is saline, with TDS concentrations up to about  $8000 \text{ mg/l}$ . Salinity is generally higher in the central, east, and southeast regions with high sulfate (up to about  $5000 \text{ mg/l}$ ) and chloride concentrations (up to about  $2600 \text{ mg/l}$ ). The objective of this study is to evaluate groundwater chemistry patterns and the processes affecting groundwater mineralization in this system. The primary results of this study could be useful for future groundwater management in the region.

\* Corresponding author. E-mail: aayaz@selcuk.edu.tr; ayla.bozdag@hotmail.com

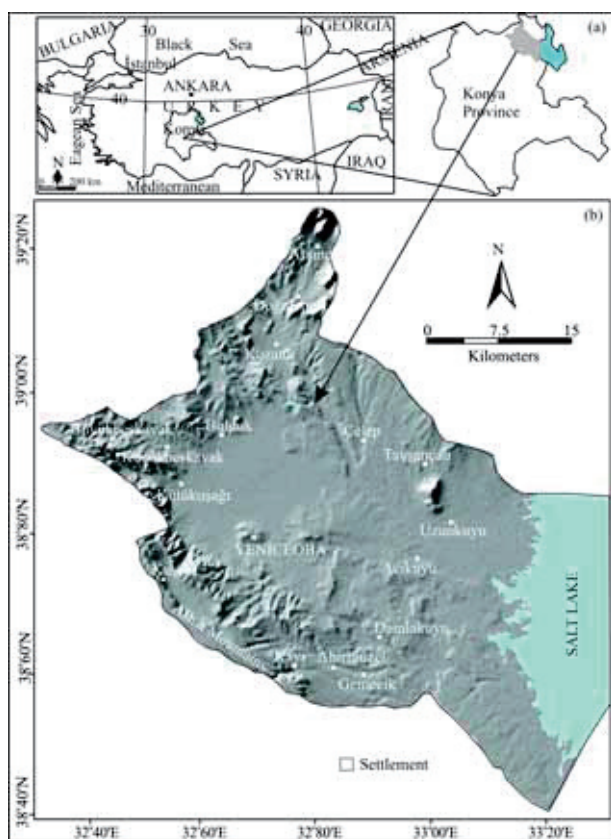


Fig. 1. The location map of the study area (a), and the Yeniceoba basin (b).

## 2 Study Area

### 2.1 General description

The Yeniceoba plain is located in the western part of the Salt Lake in northeast of Konya in the Central Anatolian region of Turkey, lying between north latitude  $38^{\circ}40' - 39^{\circ}29'$  and east longitude  $32^{\circ}31' - 33^{\circ}29'$  (Fig. 1). It covers an area of about  $1650 \text{ km}^2$  with an altitude ranging between 900 m and 1736 m above sea level (a.s.l) that decreases from the north-northwest and west-southwest to the east-southeast. The altitudes of the central and eastern parts of the study area range between 905 m and 1060 m above sea level (a.s.l). In general, the study area is characterized by an arid and semi-arid with low rainfall. The 20-year (1989–2009) average precipitation in the study area was 312.8 mm and the average temperature is  $11.69^{\circ}\text{C}$ . According to the Thorntwaite (1948) method, 93.67% of the precipitation is subjected to evapotranspiration, while the total of infiltration and surface runoff comprise only 6.33% (Bozdağ, 2010). Climatologic conditions in the region indicate that the evaporation is much higher than infiltration.

### 2.2 Geologic and hydrogeological setting

There exist a number of previous studies on regional

geology for the study area and its vicinity (e.g. Ulu et al., 1994; Dirik and Erol, 2003; Özsayın and Dirik, 2007). Six main lithostratigraphic units are recognized in the study area based upon these studies and field observations. The geological deposits range from the Triassic to Quaternary in age and include ophiolitic mélange, crystalline limestone blocks, carbonated and generally clastic sediments, volcanic and volcano-clastic units (Fig. 2). The Middle Triassic-Upper Cretaceous basement rocks (ophiolitic mélange) are composed of serpentinite, quartzite, metasandstone, gabbro, and crystalline limestone blocks. The basement rocks are unconformably overlain by the young cover units varying between the Upper Paleocene and Quaternary.

The Upper Paleocene-Lower Eocene units, composed of carbonate-cemented and medium-thick-bedded sandstone, mudstone, shale, and clay, are exposed in a narrow area in the northeastern part of the region. The Oligo-Miocene units are composed of conglomerate, sandstone, mudstone, claystone, and gypsiferous clay. The Lower Miocene volcanic deposits, crop out at the higher elevation in the north of the region, consist of andesite, basalt, volcanic breccias, and tuff. The Middle Miocene-Lower Pliocene units overlie older rocks with an angular unconformity. These units outcropping at the Asma Mountains in the southern-southwest part of the region are represented by mainly limestone, conglomerate, sandstone, clay, silt, marl and gypsiferous clay (Ulu et al., 1994).

The Plio-Quaternary units form the main aquifer system covering a large portion of the study area. The aquifer deposits characterized by vertical and lateral heterogeneity are represented by a loosely cemented conglomerate, interbedded sandstone (with varying grain sizes), siltstone, claystone, gypsiferous clay, silt, gypsum, and sulphate deposits. The conglomerates and sandstones include quartzite, chert, gabbro, serpentinite, limestone, and metamorphic rock fragments (Çemen et al., 1999). Besides, gypsum layers extend in the lateral direction within the aquifer (Ulu et al., 1994). The Quaternary alluvial sediments are located around the Yeniceoba plain and Kuşça and composed mainly of clay and sand sized material. The distribution of these units within the study area is shown in Figure 2.

The most important tectonic structure in the region is the Yeniceoba Fault Zone (YFZ) which consists of a set of parallel dip-slip faults extending in the northwest-southeast direction (Fig. 2). The YFZ controls the southern margin of Yeniceoba plain (Özsayın and Dirik, 2007).

The thickness of the alluvium around the Yeniceoba plain is a maximum of 30 m. On the other hand, the thickness of the Plio-Quaternary aquifer under the

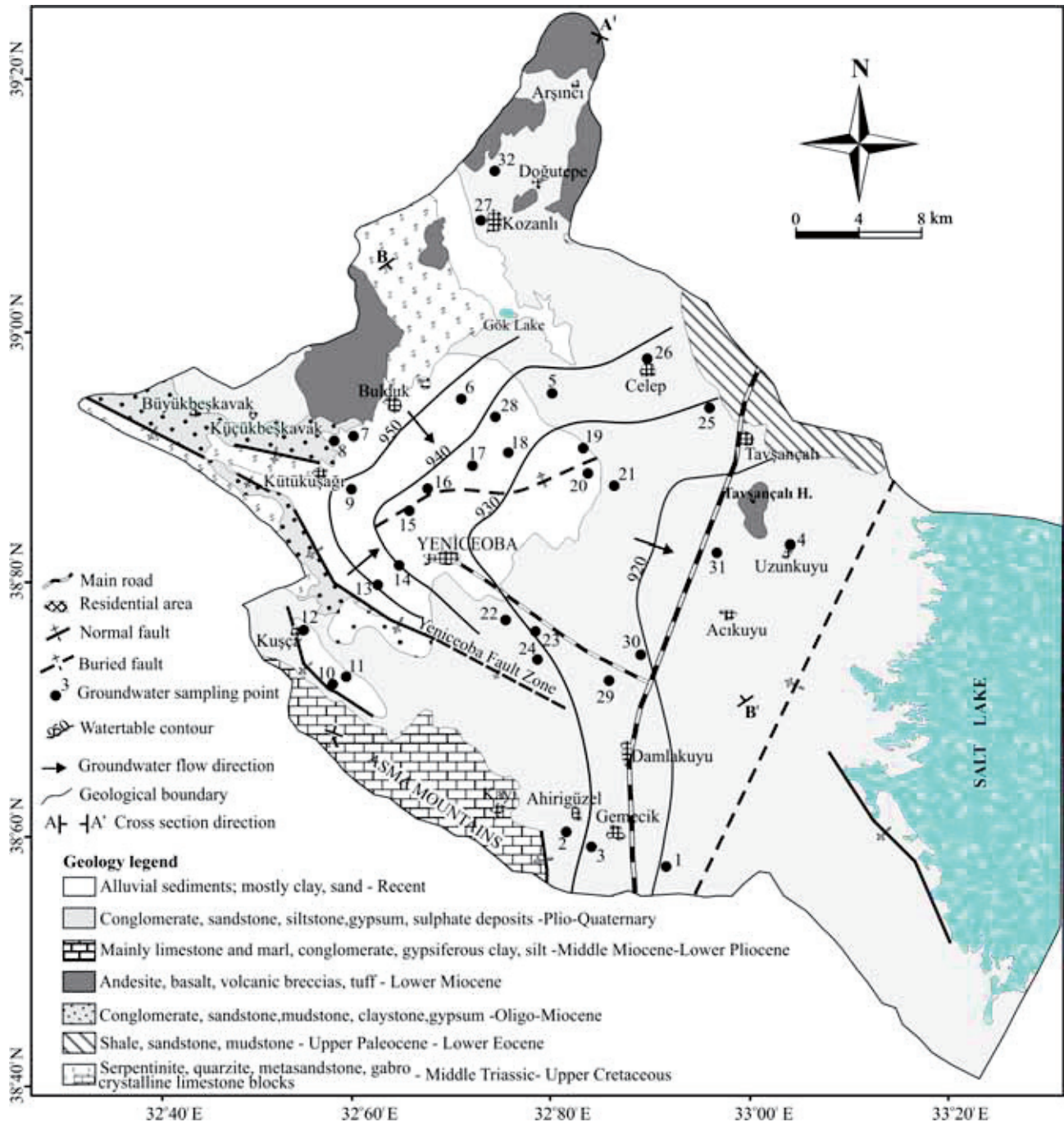


Fig.2 Geological map, water table contours and groundwater sampling points in the study area.

alluvium is between 40 and 50 m and reaches 350 m towards the east of the region. The Upper Paleocene-Lower Eocene units rest beneath the Plio-Quaternary aquifer in the north of the YFZ (DSİ, 1967). The conceptual cross sections (Fig. 3) are presented to help to understand the general geological and hydrogeological conditions in the study area. The general direction of the groundwater flow in the region is from the west, southwest and northwest to the east, namely the groundwater flows toward the Salt Lake, following the

overall basin slope (Fig. 2).

### 3 Sampling and Analytical Method

A total of thirty-two groundwater samples were collected for physicochemical analysis in October 2008. The sampling locations are shown in Fig. 2. Physicochemical parameters including EC ( $\mu\text{S}/\text{cm}$ ) and pH were measured in the field using portable measuring instruments. The bottles were washed with the water to be



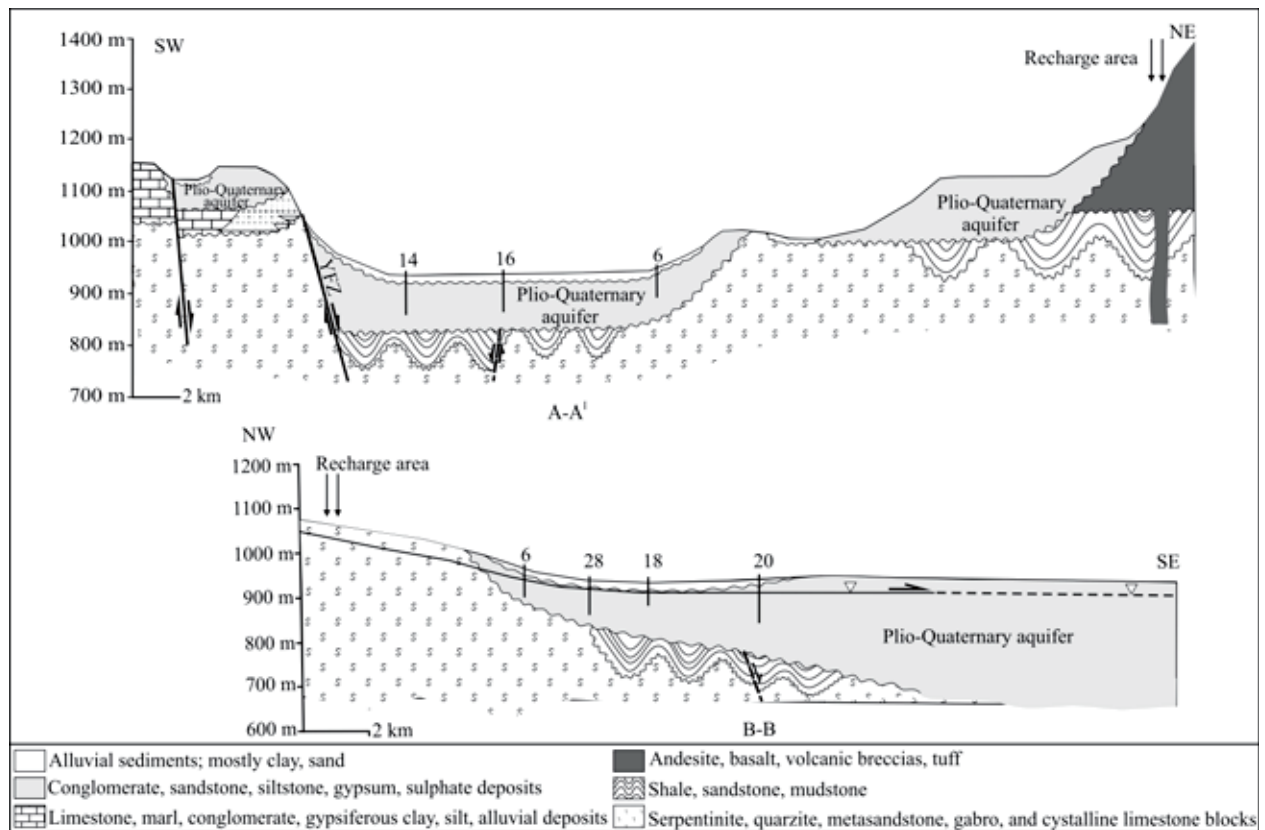


Fig. 3. Cross-sections (as shown in Fig.2). YFZ: Yeniceoba Fault Zone.

sampled before sampling. Two water samples were collected for each sample point using polyethylene bottles. The samples taken for cation analysis were acidified using pure  $\text{HNO}_3$  to prevent precipitation and preserved in refrigerator at a temperature of about  $4^\circ\text{C}$  until analysis. The parameters were determined by following standard and recommended analysis methods APHA (1995). Titrimetric methods were used to determine  $\text{HCO}_3^-$ ,  $\text{CO}_3^{2-}$ , and  $\text{Cl}^-$ , whereas  $\text{SO}_4^{2-}$  was determined gravimetrically in the laboratory.  $\text{NO}_3^-$  was determined by spectrometry [WTW SpectroFlex (6600)]. The major cations (Ca, Mg, Na and K) and Br ion were analyzed by inductively coupled plasma mass spectrophotometry (ICP-MS Enhanced) in the Acme Laboratories, Vancouver, Canada. The majority of the analyzed samples show ion balance errors within  $\pm 5\%$ , indicating the results are generally acceptable.

A total of 36 water samples for stable isotope [ $\delta^{18}\text{O}$  and  $\delta\text{D}$  (döterium)] analysis were collected from eighteen sites at two hydrological seasons [October 2008 (dry) and May 2009 (wet)]. 21 water samples for tritium ( $^3\text{H}$ ) analysis were collected from fourteen sites at two hydrological seasons. Stable isotope composition of water samples was measured by isotope ratio mass spectrometry at the Laboratory of Stable Isotopes at the University of California, Davis in the U.S. Tritium analysis were

conducted at the Technical Research and Quality Control (TAKK) Isotope Laboratories of General Directorate State Hydraulic Works (Ankara, Turkey).

The TDS concentration was calculated using the results of the chemical analyses. The distribution of major ion concentrations and correlation analysis of parameters and elements in groundwater samples were studied through the statistical and hydrogeochemical graphs. The correlation coefficient was determined to reveal the relationship between parameters by means of SPSS (version 15.0). The PHREEQC computer software was used to calculate mineral saturation index (SI) (Parkhurst and Appelo, 1999). The variations of element concentrations and parameter values in aquifer were illustrated on zoning maps through Arc GIS 10.0 (ESRI, 2010).

#### 4 Results and Discussion

The analytical results of groundwater of the study area and their computed values have been summarized along with their standard deviation in Table 1. The pH of the groundwater samples ranges from 7.20 to 8.88 with an average value of 7.87, suggesting the alkaline nature of groundwater (Table 1). The aquifer water presents wide variations in TDS and EC values that range from 443 to 7888 mg/l with an average value of 2406 mg/l, and 662



**Table 1** The statistical summary of physical and chemical parameters in groundwater

Parameter	Minimum	Maximum	Average	Standard Deviation
pH	7.2	8.88	7.87	0.32
EC	662	9305	3342	2.46
TDS	443	7888	2406	2.04
Ca	24	608	133.53	126.28
Mg	25.20	777.60	142.84	147.89
Na	33.12	1965	447.07	487.47
K	0.59	34.13	7.62	8.76
Cl	53.25	2521	582.80	627.54
HCO <sub>3</sub>	134.20	292.80	204.31	44.30
SO <sub>4</sub>	10.56	4794	885.09	1,057
NO <sub>3</sub>	2.20	948	67.57	166.62
Br	0.160	10.41	1.95	2.41
SI <sub>an</sub>	-3.20	-0.11	-1.34	0.58
SI <sub>ar</sub>	-0.32	1.27	0.22	0.38
SI <sub>cc</sub>	-0.17	1.42	0.35	0.38
SI <sub>d</sub>	-0.09	2.70	1.02	0.68
SI <sub>gyp</sub>	-2.90	0.11	-0.99	0.52
SI <sub>h</sub>	-7.19	-4.10	-5.67	0.87

Concentrations in mg/l; EC electrical conductivity ( $\mu\text{S}/\text{cm}$ ); Log Saturation Index (SI) of calcite (cc), aragonite (ar), dolomite (d), gypsum (gyp), anhydrite (an), halite (h).

to 9305  $\mu\text{S}/\text{cm}$  with an average value of 3342  $\mu\text{S}/\text{cm}$ , respectively. The TDS and EC values of the groundwater increase along the direction of groundwater flow from the recharge in high topographic areas located in the north, west, and southwest to discharge areas in low topographic areas in the east. However, there is no specific change in the horizontal or vertical directions due to the heterogeneous nature of the aquifer (Fig. 4a, b). The TDS values (well numbers 4, 29, 30 and 31) located in the east of the study area are relatively lower when compared to TDS values around Yeniceoba (Fig. 2). The depth of wells ranges from 50 to 90 m around Yeniceoba and from 18 to 30 m in the east of the study area. High TDS values of the

groundwater samples around Yeniceoba may result from long residence time of groundwater and associated enhanced water-rock interaction.

#### 4.1 Geochemical characteristics and origin of groundwater mineralization

The groundwater samples show a wide variability in the concentrations of Ca, Mg, Na, Cl and SO<sub>4</sub>, which range from 24 to 608 mg/l, 25.20 to 777.60 mg/l, 33.12 to 1965 mg/l, 53.25 to 2521 mg/l and 10.56 to 4794 mg/l, respectively. Conversely, concentrations of HCO<sub>3</sub> and K show a narrow range as given in Table 1 varying between 134.20 and 292.80 mg/l; 0.59 and 34.13 mg/l, respectively. The samples' scattering in Piper (1944) diagram is due to heterogeneity in aquifer deposits (Fig. 5). The relative occurrences of both cations and anions in the groundwater samples give a wide range of hydrogeochemical water types from Mg-Ca-HCO<sub>3</sub>-(Cl), Mix-type, Mg-Na-(Ca)-SO<sub>4</sub>-Cl, Na-Mg-SO<sub>4</sub>-Cl, and Na-Cl or Na-Cl-SO<sub>4</sub>. The hydrogeochemical water type varies from Mg-Ca-HCO<sub>3</sub> in the recharge area in the north (nearby mountains) to Mg-Na-(Ca)-SO<sub>4</sub>-Cl in the west and around Yeniceoba, and to Na-Cl/ Na-Cl-SO<sub>4</sub> in the east (Fig. 6).

In order to better understand the processes leading to the observed mineralization, bivariate diagrams of chemical constituents in the analyzed groundwater samples were used. The Ca and Mg contents of the majority of the groundwater samples are in excess of the carbonate dissolution line and at the same time lacking of any correlation with HCO<sub>3</sub> content (Table 2, Fig. 7a). In addition, the sum of Ca and Mg ions are strongly

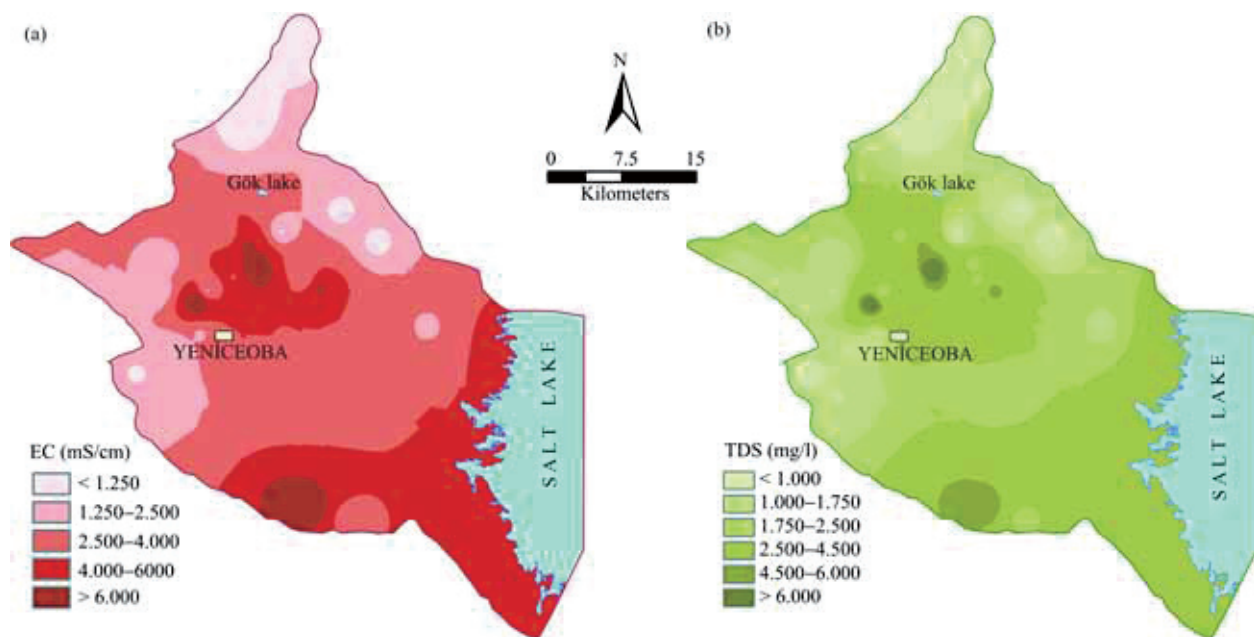


Fig. 4. The spatial distribution maps. (a), EC ( $\mu\text{S}/\text{cm}$ ); (b), TDS (mg/l).

**Table 2 Correlation coefficients between various parameters in the groundwater samples**

Parameter	pH	EC	TDS	Ca	Mg	Na	K	Cl	HCO <sub>3</sub>	SO <sub>4</sub>	NO <sub>3</sub>	Br
pH	1.000											
EC	0.257	1.000										
TDS	0.203	0.995	1.000									
Ca	-0.026	0.779	0.789	1.000								
Mg	-0.216	0.732	0.761	0.896	1.000							
Na	0.462	0.888	0.873	0.448	0.350	1.000						
K	0.579	0.487	0.442	0.236	0.015	0.613	1.000					
Cl	0.628	0.784	0.736	0.450	0.212	0.902	0.721	1.000				
HCO <sub>3</sub>	-0.020	0.249	0.254	-0.050	-0.035	0.393	0.415	0.285	1.000			
SO <sub>4</sub>	-0.172	0.823	0.864	0.807	0.936	0.547	0.079	0.298	0.098	1.000		
NO <sub>3</sub>	-0.004	-0.068	-0.078	-0.105	-0.075	-0.055	-0.209	-0.106	-0.160	-0.032	1.000	
Br	0.125	0.759	0.756	0.388	0.428	0.789	0.274	0.643	0.279	0.578	-0.049	1.000

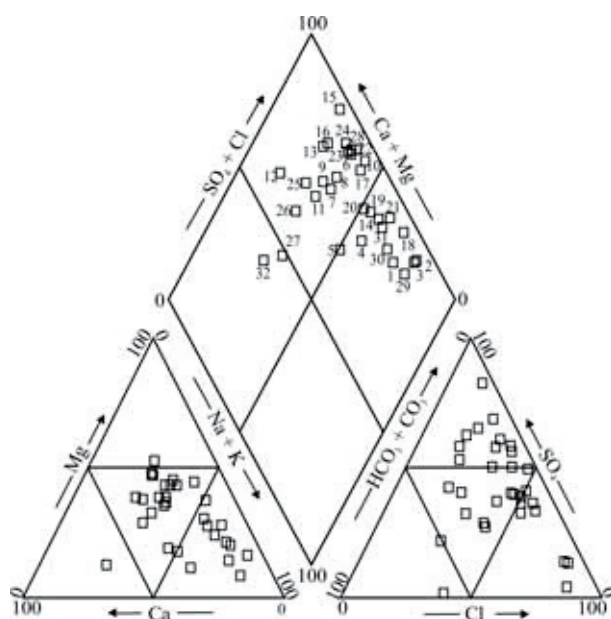


Fig. 5. The piper diagram for the groundwater samples of the study area.

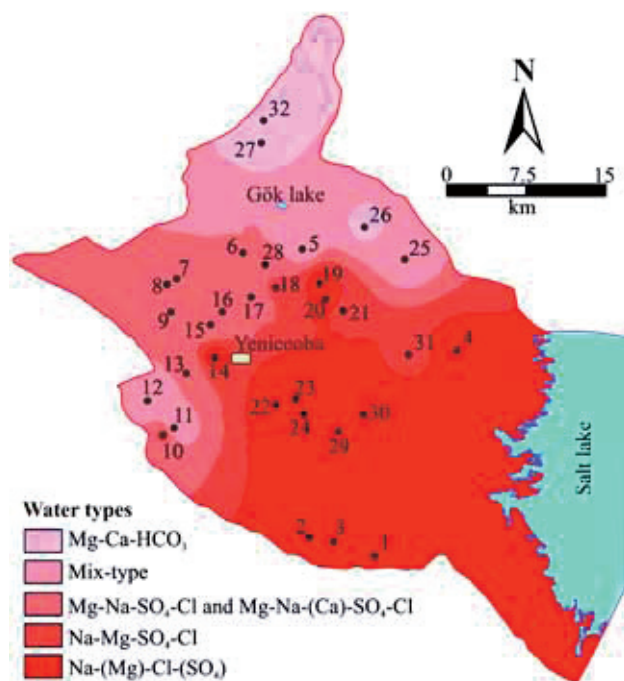


Fig. 6. Zoning map of hydrogeochemical facies in the study area.

correlated with SO<sub>4</sub> content ( $r^2=0.84$ ) which points to dissolution of evaporitic minerals as a major source of these ions in groundwater samples. However, some water samples are placed above line 1:1 which is due to an increase in Ca and Mg versus SO<sub>4</sub> (Fig. 7b). This increase in Ca and Mg indicates the contribution of another geochemical process that affects cation contents. The sources of Ca and Mg in groundwater can also be deduced from the  $m(\text{Mg}+\text{Ca})/m\text{HCO}_3$  ratio. If Ca and Mg originated solely from the dissolution of carbonates in the aquifer materials and from the weathering of accessory pyroxenes and amphibole minerals, this ratio would be about 0.5 (Sami, 1992; Taheri Tizro and Voudouris, 2008). However, this ratio is higher than 0.5 in the groundwater in studied aquifer (Fig. 7c). High values of Mg/Cl and Ca/Cl ratios in the low salinity samples probably reflect weathering of carbonates (e.g. calcite, and dolomite), silicates minerals such as ferromagnesian minerals (e.g. olivine, biotite, hornblend), and Ca silicate minerals (e.g. plagioclase feldspar) in the host rocks in the recharge regions and rock fragments within the aquifers. Mg/Cl and Ca/Cl ratios increase with increasing salinity probably due to the reverse ion exchange between Mg, Ca and Na ions (Fig. 7d, e).

Along flow path, the groundwater contacts with gypsum deposits. As gypsum has a higher solubility than calcite and the conditions are appropriate for gypsum dissolution (generally negative saturation index, Fig 7f), gypsum dissolution ( $\text{CaSO}_4 \cdot 2\text{H}_2\text{O} + 2\text{HCO}_3 \rightarrow \text{CaCO}_3 + \text{SO}_4 + \text{H}_2\text{O} + \text{CO}_2$ ) enhances calcium and sulfate concentrations. By further dissolution of gypsum and by an increase in Ca concentration through common ion effect process, calcite is precipitated (Edmunds and Shand, 2008), therefore controls the amount of hydrogencarbonate in water (Helena et al., 1999). Saturation index (SI) shows a progressive saturation in gypsum and anhydrite with an increase in SO<sub>4</sub> concentrations (Fig. 7f). Majority of the samples are saturated or close to saturation with respect to calcite and dolomite (Table 2), suggesting that precipitation of these minerals may limit Ca concentration

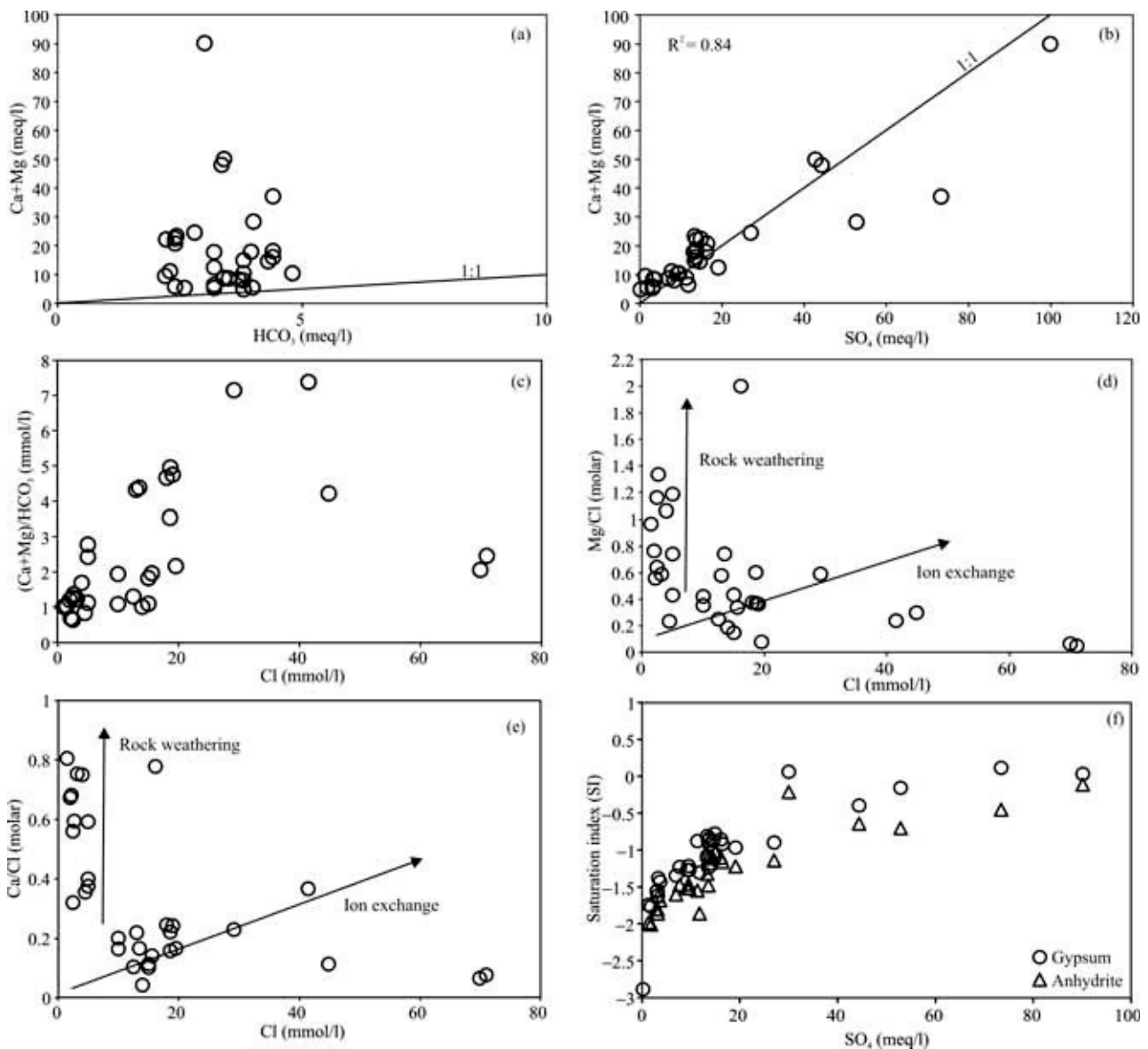


Fig. 7 Hydrochemical relationships (a) Ca + Mg -  $\text{HCO}_3$ ; (b) Ca + Mg -  $\text{SO}_4$ ; (c)  $(\text{Ca} + \text{Mg})/\text{HCO}_3$  - Cl; (d) Ca/Cl-Cl; (e) Mg/Cl-Cl; (f)  $(\text{SI}_{\text{gypsum}} \text{ and } \text{SI}_{\text{anhydrite}})$  -  $\text{SO}_4$

in the groundwater. Dolomite dissolution is unlikely to be a significant source of magnesium in the aquifer water as there is no correlation between Mg and  $\text{HCO}_3$ , implying that main sources of Mg in the Plio-Quaternary aquifer are the weathering of silicate minerals in the host rocks and in the rock fragments within the aquifer system and reverse ion exchange process.

The relationship between the concentrations of Na and Cl has been widely used to identify the mechanism of salinity in arid and semi-arid regions (Dixon and Chiswell, 1992; Magaritz et al., 1981; Sami, 1992; Hamid and Kayhomayoon, 2013). Despite the strong correlation between Na and Cl ions ( $r^2 = 0.90$ ) there is some variation in their ratios (Table 2). The ion ratio of  $\text{Na}/(\text{Na} + \text{Cl}) < 0.5$  shows the decrease of Na concentration in the

groundwater samples. The cause of sodium reduction in the groundwater in the study area is reverse ion exchange process. When saline groundwater enters an environment with a lower degree of groundwater salinity, Na is replaced by Ca and Mg ions (Fetter, 2000). Thus, Mg-Na- $\text{SO}_4$ -Cl or Mg-Na-(Ca)-Cl- $\text{SO}_4$  water types have been derived in the west part of the study area. In contrast, the ion ratio of  $\text{Na}/(\text{Na} + \text{Cl}) > 0.5$  have been obtained in the samples around Yeniceoba with Na-(Mg)- $\text{SO}_4$ -Cl water type (Fig. 8). This ion ratio can be explained by ion exchange reactions with clay minerals (Hounslow, 1995; Faye et al., 2005; Guendouz et al., 2006; Kortatsi, 2007) within aquifer deposits. Further, the positive correlation ( $r^2 = 0.55$ ) between  $\text{SO}_4$  and Na ions suggests that some of these ions may be derived from the dissolution of sulfur-



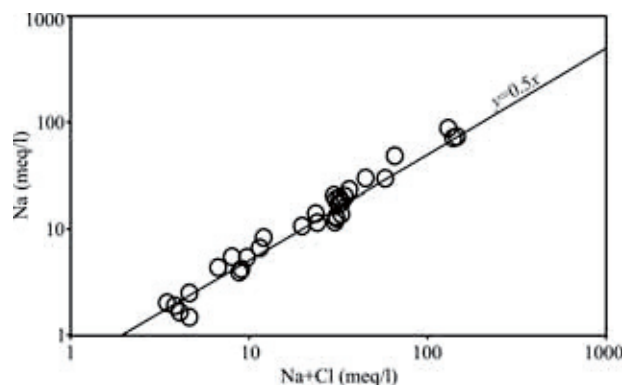


Fig. 8. Plot diagram of Na versus Na+Cl.

bearing minerals such as sodium sulfate minerals.

The Cl/Br ratio is suitable for identifying different sources of groundwater salinization (Davis et al., 2001). The Cl/Br ratio in groundwater samples varies from 105.65 mg/l to 1305.65 mg/l with an average value of 448.66 mg/l. The values of Cl/Br ratio in groundwater samples are due to the difference in Cl and Br concentrations. Generally, Cl/Br ratio highly exceeding 200 suggests the existence of Cl sources in the aquifer (Fig. 9), which may be either natural or anthropogenic (Davis et al., 2001). In addition, the high Cl/Br ratios of groundwater in the Plio-Quaternary aquifer indicate that the elevated mineralization is due to the dissolution of evaporitic minerals (Kohfahl et al., 2008). The bromide concentration of groundwater in the study area increases from 0.16 mg/l at the high topographic areas to 3.94 mg/l in the flat area around Yeniceoba and towards the Salt Lake, except for well numbers 18 and 28 in which the bromide concentration of the samples are up to 10.41 mg/l and 7.52 mg/l, respectively. Due to the large ionic size of Br, its ion is not compiled in the halite mineral structure, and in this way halite dissolution produces an increase in Cl/Br ratios with increasing Cl concentrations (Cartwright et al., 2006). This tendency can be seen in Fig. 9. Cl/Br ratios of the groundwater samples show some evidence of ongoing halite dissolution as one cause of increasing salinity, and the low salinity groundwater with high Cl/Br

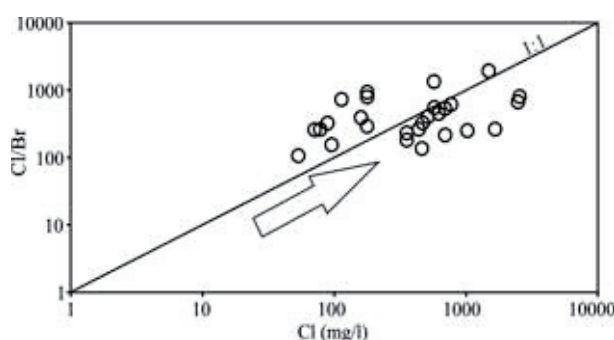


Fig. 9. Scatter diagram of Cl/Br (molar) versus Cl (mmol).

ratios can also be interpreted as having undergone halite dissolution. However, halite dissolution must be relatively minor as halite has Cl/Br ratios of  $10^4$ – $10^5$  (e.g., Cartwright et al., 2004).

The nitrate concentrations in water samples varies from 2.20 mg/l (well no. 7) to 948 mg/l (well no: 31) with an average value of 67.56 mg/l.  $\text{NO}_3$  comprises 3.88 % of total anions and does not vary in relative abundance with salinity and there is also no correlation between nitrate and any other ions of groundwater samples in the Plio-Quaternary aquifer (Table 2). Furthermore, the contents of  $\text{NO}_3$  in well waters in agricultural and residential areas are higher than those found in high topographic areas. These results reveal that changes in land use and other human activities have led to  $\text{NO}_3$  enrichment. In addition, Figure 10 shows that nitrate concentrations tend to be higher in the shallower wells, which is likely to show that these wells are more affected by agricultural activities including the use of fertilizers and/or domestic effluents such as sewage leakage and manure piles in the region.

#### 4.2 Isotopic composition of waters

Eighteen water samples in October 2008 (in dry season) and in May 2009 (in wet season) were analyzed for hydrogen and oxygen stable isotopes. Individual data points are listed in Table 3 and shown in Fig. 11. The measured stable isotope composition of the groundwater

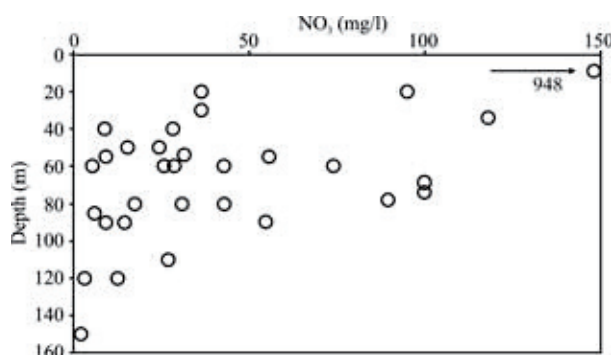


Fig. 10. Variation in  $\text{NO}_3$  concentrations with depth.

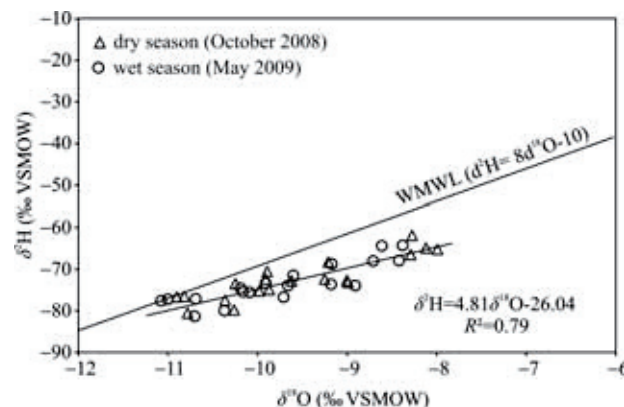


Fig. 11.  $\delta^{18}\text{O}$ - $\delta\text{D}$  diagram of the analysed groundwater samples.

**Table 3 Isotopic composition of groundwater samples in the study area**

Sample No.	$\delta^2\text{H}_{(d)}$	$\delta^{18}\text{O}_{(d)}$	$\delta^2\text{H}_{(w)}$	$\delta^{18}\text{O}_{(w)}$	TU <sub>(d)</sub>	TU <sub>(w)</sub>	Well Depth
2	-79.81	-10.26	-79.99	-10.37	0.00	0.00	120
4	-65.29	-7.99	-64.28	-8.38	0.10	0.12	30
6	-72.71	-9.00	-73.67	-9.18	0.00	n.m.	60
9	-70.21	-9.89	-71.50	-9.60	0.25	n.m.	60
10	-77.48	-10.36	-75.82	-9.85	0.80	n.m.	55
12	-76.66	-10.90	-77.38	-11.13	n.m.	n.m.	80
13	-72.8	-9.62	-73.36	-9.91	0.00	n.m.	60
15	-73.18	-8.99	-73.96	-8.91	0.22	n.m.	50
16	-76.59	-10.82	-77.12	-10.69	n.m.	n.m.	80
18	-75.20	-9.98	-75.60	-10.09	0.00	0.00	50
20	-74.93	-9.87	-75.46	-10.16	n.m.	n.m.	90
21	-73.45	-10.25	-74.58	-10.19	0.00	0.00	80
22	-80.59	-10.78	-81.31	-10.70	0.00	0.00	90
25	-61.87	-8.28	-64.03	-8.61	2.75	n.m.	34
26	-68.32	-9.21	-68.78	-9.17	n.m.	n.m.	60
27	-72.40	-9.91	-73.92	-9.66	0.00	0.00	110
29	-64.89	-8.12	-67.94	-8.42	7.65	8.28	20
31	-66.49	-8.29	-68.05	-8.71	3.12	n.m.	18

Note: n.m., not measured; d: dry season (October 2008); w: wet season (May 2009).

samples is plotted on a  $\delta^{18}\text{O}$ - $\delta\text{D}$  diagram, together with reference to World Meteoric Water Line (WMWL;  $\delta\text{D} = 8\delta^{18}\text{O} + 10$ ; Craig, 1961) (Fig. 11).

Oxygen-18 content in the wet and dry seasons varies from  $-8.38$  to  $-11.13\text{‰}$  with an average of  $-9.72\text{‰}$ , and from  $-7.99$  to  $-10.90\text{‰}$  with an average of  $-9.58\text{‰}$ , respectively. Deuterium content in wet and dry seasons varies from  $-64.03$  to  $-81.31\text{‰}$  with an average of  $-73.26\text{‰}$ , and from  $-61.87$  to  $-80.59\text{‰}$  with an average of  $-72.38\text{‰}$ , respectively (Table 3). Isotopic composition of groundwater samples in the dry season is slightly enriched with heavy isotopes because of evaporation.

Groundwater with a  $\delta\text{D}/\delta^{18}\text{O}$  slope of  $\sim 8$  indicates the origin from meteoric water with minimal post-precipitation effects, whereas a slope  $< 8$  may reflect evaporation during or after rainfall (Gat and Dansgaard, 1972; Clark and Fritz, 1997). In this study, the graph of  $\delta^{18}\text{O}$  versus  $\delta\text{D}$  (Fig. 11) shows an evident inclination with a linear relationship ( $y = 4.81x - 26.04$ ;  $r^2 = 0.79$ ). This low

slope (4.81) suggests that the groundwater has undergone evaporation processes. Evaporation effects are seen notably on the samples taken from shallower wells (no. 4, 25, 29 and 31). As seen in Fig. 12a and b, the samples belonging to shallower wells shift towards heavier values of  $\delta^{18}\text{O}$  and  $\delta\text{D}$  as a result of the intense evaporation.

The Deuterium-excess ( $d$ -excess), used as a proxy for identifying secondary processes that influence the atmospheric vapor content in the evaporation-condensation cycle in nature (Craig, 1961; Dansgaard 1964), indicates the evaporation effect on the physicochemical characteristics of water. Low  $d$ -excess values can reflect high humidity in the source region, while high  $d$ -excess values can result from lower humidity in the source region (Clark and Fritz, 1997). According to Cappa et al. (2003), water vapor with low  $d$  values is likely to occur at high humidity, in high  $d$  values of ambient air masses, and/or low  $d$  values of evaporating waters. The  $d$ -excess value of the samples ranges from  $10.55$  to  $-2.68\text{‰}$  and  $11.66$  to

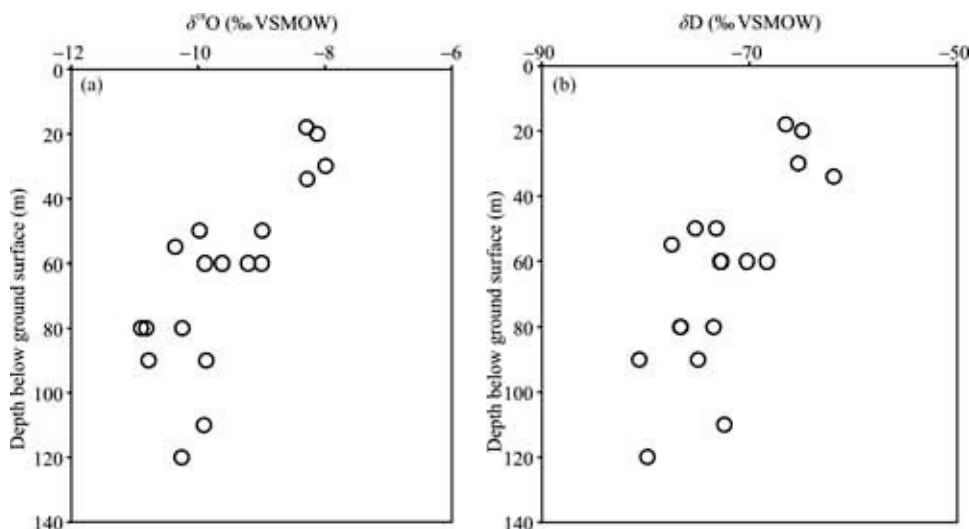


Fig. 12. Depth distribution of  $\delta^{18}\text{O}$  (a) and  $\delta\text{D}$  of groundwater samples (b).

−1.37‰ in dry and wet seasons, respectively. Generally, *d*-excess values in the dry season are lower than those in the wet season which may be related to a greater degree of evaporation in the dry season (Ghalib and Söğüt, 2014; Tiping et al., 2014). To better understand the processes affecting the isotopic signatures of oxygen and hydrogen,  $\delta^{18}\text{O}$  versus *d*-excess have been plotted for two seasons (Fig. 13) which shows a negative correlation between  $\delta^{18}\text{O}$  and *d*-excess for the groundwater samples, confirming the effect of evaporation on groundwater. Thus, the evaporation process contributes to the increase in groundwater mineralization. Diaw et al. (2012) asserted that the enriched stable isotopes values associated with relatively low *d*-excess values may be interpreted with the evaporation during the recharge processes. The similar results have been obtained in the Plio-Quaternary groundwater.

Tritium ( $^3\text{H}$ , half-life time 12.43 years) is widely used as a radioisotope tracer to identify the modern recharge and to estimate groundwater residence time (Fontes, 1883; Yurtsever, 1983; Lee et al., 2011). Because the tritium input function is coupled with the H-bomb peak of the 1960s (1952–1962), groundwater with high tritium concentrations of >30 TU indicates a recharge during and after the 1960s. Recent precipitation and recharged groundwater in the northern hemisphere has tritium concentrations up to 9 TU (IAEA/WMO, 2006). Groundwater containing  $^3\text{H}$  values <1 TU is often classified as sub-modern (pre-1960s) (Clark and Fritz, 1997).

Tritium contents of 14 samples are given in Table 3 for both dry and wet seasons. More than 80% of the samples in both seasons have lesser values than 1 TU (between 0.00 and 0.80 TU). Very low values of tritium even for shallow groundwater suggests minor contribution of modern recharge, thus indicating groundwater residence times of more than three or four decades. However, higher values ranging from 2.75 to 7.65 TU are measured in a few shallower wells (well no. 25, 29 and 31) showing that the

groundwater recharges by recent precipitation. In summary, tritium contents of the Plio-Quaternary groundwater are less than 1 TU and homogeneous suggesting a minor contribution of recent recharge and groundwater residence times of more than three or four decades.

## 5 Conclusion

The Plio-Quaternary aquifer water has a relatively wide range of TDS, reaching nearly 8,000 mg/l. The mineralization of groundwater increases along the direction of its flow from the recharge in high topographic areas located in the north, west, and southwest to discharge areas in low topographic areas in the east. The dominant hydrogeochemical facies of groundwater in the Plio-Quaternary aquifer varies from Mg-Ca- $\text{HCO}_3$  in the recharge area (nearby mountains) to Mg-Na-(Ca)- $\text{SO}_4$ -Cl in the central area and to Na-Cl- $\text{SO}_4$  or Na-Cl towards the Salt Lake.

The results reveal that the hydrogeochemical properties of the Plio-Quaternary aquifer are principally controlled by rock/water interactions including dissolution of evaporitic minerals (halite, gypsum, sulfur-bearing minerals such as sodium sulfate minerals), silicate weathering, precipitation/dissolution of carbonates, ion exchange, and evaporation. According to Cl/Br ratio (>300 mg/l) in the study aquifer, it can be concluded that dissolution of evaporitic minerals in aquifer contributes significantly to the observed mineralization of groundwater.

The stable isotopic compositions indicate that the groundwater of Plio-Quaternary aquifer was influenced by evaporation during recharge. In most groundwater during dry and wet seasons, tritium contents are less than 1 TU and homogeneous which suggests a very low contribution from modern recharge, therefore indicating mostly old groundwater with minimal recharge occurring in recent decades and groundwater residence times of more than three or four decades. Based on isotope data, it can be concluded that evaporation and long groundwater residence times also contribute to the high mineralization of the Plio-Quaternary groundwater.

## Acknowledgments

This study was financially supported by Selçuk University Scientific Research Projects (BAP) (Project no. 07101034) (Konya, Turkey).

Manuscript received Aug. 21, 2014  
accepted June 25, 2015  
edited by Fei Hongcai

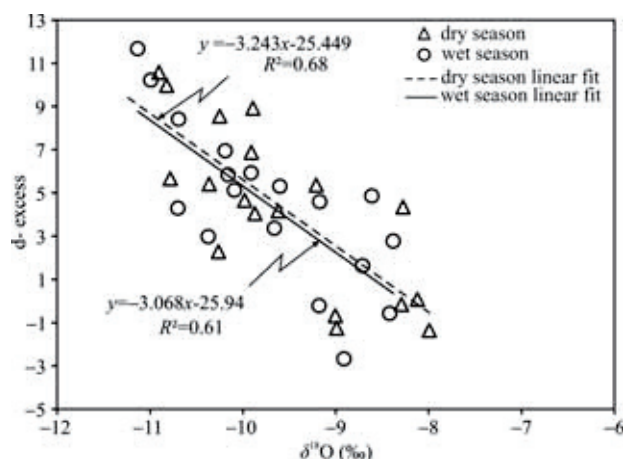


Fig. 13.  $\delta^{18}\text{O}$  versus *d*-excess plots for the groundwater samples.



## References

- Al-Charideh, A., 2012. Geochemical and isotopic characterization of groundwater from shallow and deep limestone aquifers system of Aleppo basin (north Syria). *Environmental Earth Sciences*, 65: 1157–1168.
- APHA 1995. *Standard methods for the examination of water and wastewater*. (19th ed.). American Public Association, Washington, DC.
- Bozdağ, A., 2010. *Investigation of hydrogeological, hydrochemical and isotopic characteristic of the Cihanbeyli (Konya) and surrounding area*. PhD Thesis, Institute of Science, Selçuk University, Konya, 299 p.
- Cappa, C.D., Hendricks, M.B., DePaolo, D.J., and Cohen, R.C., 2003. Isotopic fractionation of water during evaporation. *Journal of Geophysical Research-Atmospheres*, 108 (D16): 1–10.
- Cartwright, I., Weaver, T.R., Fulton, S., Nichol, C., Reid, M., and Cheng, X., 2004. Hydrogeochemical and isotopic constraints on the origins of dryland salinity, Murray Basin, Victoria, Australia. *Applied Geochemistry*, 19: 1233–1254.
- Cartwright, I., Weaver, T.R., and Fifield, L.K., 2006. Cl/Br ratios and environmental isotopes as indicators of recharge variability and groundwater flow. An example from the southeast Murray Basin, Australia. *Chemical Geology*, 231: 38–56.
- Clark, I.D., and Fritz, P., 1997. *Environmental isotopes in hydrogeology*, Lewis Publishers, New York, p 328.
- Cook, P., and Herczeg, A.L., (eds) 2000. *Environmental tracers in subsurface hydrology*. Kluwer, New York.
- Craig, H., 1961. Isotopic variations in meteoric waters. *Science*, 133: 1702–3.
- Çemen, İ., Gönçüoğlu, M.C., and Dirik, K., 1999. Structural Evolution of the Tuzgölü Basin in Central Anatolia, Turkey. *The Journal of Geology*, 107 (6): 693–706.
- Dansgaard, W., 1964. Stable isotopes in precipitation. *Tellus*, 16: 436–468.
- Davis, S.N., Cecil, L., Zreda, M., and Moysey, S., 2001. Chlorine-36, bromide and the origin of spring water. *Chemical Geology*, 179(1–4): 3–16.
- Diaw, M., Faye, S., Stichler, W., and Maloszewski, P., 2012. Isotopic and geochemical characteristics of groundwater in the Senegal River delta aquifer: implication of recharge and flow regime. *Environmental Earth Sciences*, 66(4): 1011–1020.
- Dirik, K., and Erol, O., 2003. Tectonomorphologic evolution of Tuzgölü and surrounding area, Central Anatolia-Turkey. *Turkish Association of Petroleum Geologists Special Publication*, 5: 27–46.
- Dixon, W., and Chiswell, B., 1992. The use of hydrochemical sections to identify recharge areas and saline intrusions in alluvial aquifers, southeast Queensland, Australia. *Journal of Hydrology*, 130: 299–338.
- DSİ (General Directorate of State Hydraulic Works) 1967. *IV. Region, Kulu-Cihanbeyli Plains Geophysical Resistivity Survey Report*, Ankara.
- Edmunds, W.M., Guendouz, A., Mamou, A., Moulla, A., Shand, P., and Zouari, K., 2003. Groundwater evolution in the Continental Intercalaire aquifer of southern Algeria and Tunisia: trace element isotopic indicators. *Applied Geochemistry*, 18: 805–822.
- Edmunds, W.M., 2005. Contribution of isotopic and nuclear tracers to study of groundwater. In: Aggarwal, P.K., Gat, J.R., and Froehlich, K.F.O. (eds.), *Isotopes in the water cycle: past, present and future of a developing science*. IAEA, Springer, Netherlands, p 381.
- Edmunds, W.M., and Shand, P., 2008. *Natural groundwater quality*. Blackwell, Oxford.
- ESRI 2010. *ArcGIS 10 The Principles of Geostatistical Analysis*. ArcGIS 10.
- Faye, S., Maloszewski, P., Stichler, W., Trimborn, P., Faye, S.C. and Gaye, C.B., 2005. Groundwater salinization in the Saloum (Senegal) delta aquifer: minor elements and isotopic indicators. *Science of the Total Environment*, 343(1–3): 243–259.
- Fetter, C.W., 2000. *Applied hydrogeology*. CBS Publishers, New Delhi.
- Fontes, J.C., 1983. *Dating of groundwater*. Guidebook on nuclear techniques. Technical Report Series no 91. IAEA, Vienna.
- Gat, J.R., and Dansgaard, W., 1972. Stable isotope survey of the freshwater occurrence in Israel and northern Jordan rift valley. *Journal of Hydrology*, 16: 177–21.
- Ghalib, H.B., and Söğüt, A.R., 2014. Environmental Isotopic Characterization of Groundwater and Surface Water in Northeast Missan Province, South Iraq. *Acta Geologica Sinica (English Edition)*, 88(4): 1227–1238.
- Guendouz, A., Moulla, A.S., Edmunds, W.M., Zouari, K., Shand, P., and Mamou, A., 2003. Hydrogeochemical and isotopic evolution of water in the Complex Terminal aquifer in the Algerian Sahara. *Journal of Hydrology*, 11: 483–495.
- Guendouz, A., Moulla, A.S., Remini, B., and Michelot, J.L., 2006. Hydrochemical and isotopic behaviour of a Saharan phreatic aquifer suffering severe natural and anthropic constraints (case of Oued-Souf Region, Algeria). *Hydrogeology Journal*. 14: 955–968.
- Hamid, R.N., Kayhomayoon, Z., 2013. Source of salinity in the groundwater of Lenjanat Plain, Isfahan, Iran. *Environmental Earth Sciences*, 68: 413–427.
- Helena, B.A., Vega, M., Barrado, E., Pardo, R., and Fernandez, L., 1999. A case of hydrochemical characterization of an alluvial aquifer influenced by human activities. *Water, Air & Soil Pollution*, 112: 365–387.
- Hounslow, A.W., 1995. *Water quality data, analysis and interpretation*. Lewis Publication, Boca Raton.
- IAEA/WMO 2006. *Global network of isotopes in precipitation*. The GNIP Database. <http://www.iaea.org/water>
- Kohfahl, C., Rodriguez, M., Fenk, C., Christian, M., Benavente, J., Hubberten, H., Meyer, H., Paul L., Knappe, A., Lopez-Geta, J.S., and Pekdeğer, A., 2008. Characterising flow regime and interrelation between surface-water and groundwater in the Fuente de Piedra salt lake basin by means of stable isotopes, hydrogeochemical and hydrologic data. *Journal of Hydrology*, 351: 170–187.
- Kortatsi, B.K., 2007. Hydrochemical framework of groundwater in the Ankobra Basin, Ghana. *Aquatic Geochemistry*, 13: 41–74.
- Lee, J., Jung, B., Kim, J.H., Ko, K.S., and Chang, H.W., 2011. Determination of groundwater flow regimes in underground storage caverns using tritium and helium isotopes. *Environmental Earth Sciences*, 63: 763–770.
- Magaritz, M., Nadler, A., Koyumdjisky, H., and Dan, N., 1981. The use of Na/Cl ratio to trace solute sources in a semiarid zone. *Water Resources Research*, 17: 602–608.

- Özsayın, E., and Dirik, K., 2007. Quaternary activity of the Cihanbeyli and Yeniceoba fault zones. İnönü-Eskişehir Fault System, Central Anatolia. *Turkish Journal of Earth Sciences*, 16: 471–492.
- Parkhurst, D.L., and Appelo, C.A.J., 1999. *User's guide to PHREEQC (Version 2) -A computer program for speciation, batch-reaction, one-dimensional transport, and inverse geochemical calculations*. Water-Resources Investigations, Report 99-4259, Denver, Co, USA, 312.
- Piper, A.M., 1944. A graphic procedure in the geochemical interpretation of water analysis. *Transactions-American Geophysical Union*, 25: 914–923.
- Sami, K., 1992. Recharge mechanisms and geochemical processes in a semi-arid sedimentary basin, Eastern Cape, South Africa. *Journal of Hydrology*, 139: 27–48.
- Taheri Tizro, A., and Vouduris, K.S., 2008. Groundwater quality in the semi-arid region of the Chahardouly basin, West Iran, *Hydrological Processes*, 22: 3066–3078.
- Thorntwaite, W.C., 1948. An approach toward a rational classification of climate. *Geographical Review*, 38: 55–94.
- Tiping D., Jianfei, G., Shihong, T., Guoyu, S., Feng, C., Chengyu, W., Xurong, L., and Dan, H., 2014. Chemical and Isotopic Characteristics of the Water and Suspended Particulate Materials in the Yangtze River and Their Geological and Environmental Implications, *Acta Geologica Sinica* (English Edition), 88(1): 276–360.
- Ulu, Ü., Bulduk, A.K., Ekmekçi, E., Karakaş, M., Öcal, H., Abbas, A., Saçlı, L., Taşkıran, M.A., Adır, M., Sözeri, Ş., and Karabıyıköğlü, M., 1994. Geology of İnlice-Akkise and Cihanbeyli-Karapınar Area: *General Directorate of Mineral Research and Exploration Comp. Rap. No: 9720*, Ankara (in Turkish).
- Yurtsever, Y., 1983. *Models for tracer data analysis*. In: Guidebook on nuclear techniques in hydrology. Technical Reports, Series no 91.IAEA,Vienna.

#### About the first author

Ayla Bozdağ graduated from Department of Geological Engineering, Selçuk University and received her Ph.D. at the same university. Her research interests include hydrogeochemistry, hydrogeology and environmental geology.